

Supporting Information for

Zero-dimensional mixed-cation hybrid lead halides with broadband emissions

Mirosław Mączka,* Dawid Drozdowski, Dagmara Stefańska, Anna Gaĝor

*Institute of Low Temperature and Structure Research, Polish Academy of Sciences, ul. Okólna 2,
50-422 Wrocław, Poland*

e-mail: m.maczka@intibs.pl

Table S1. Experimental and refinement details of Cs₂MHy₂PbX₆ (X = Br, I) at 295 K.

	Cs ₂ MHy ₂ PbBr ₆	Cs ₂ MHy ₂ PbBr ₃ I ₃	Cs ₂ MHy ₂ PbI ₆
Crystal data			
Crystal system, space group	Orthorhombic, <i>Cmce</i>		
<i>a</i> , <i>b</i> , <i>c</i> (Å)	14.280(4), 12.876(4), 10.772(4)	14.666(4), 13.245(4), 10.986(4)	15.154(5), 13.629(4), 11.444(4)
<i>V</i> (Å ³)	1980.7(11)	2134.1(12)	2363.6(13)
<i>Z</i>	4		
Δ <i>d</i> × 10 ⁻⁵ , σ ²	0.12, 7.67	29.9, 7.64	1.1, 7.25
μ (mm ⁻¹)	24.23	21.21	18.00
Crystal size (mm)	0.26 × 0.22 × 0.16	0.26 × 0.19 × 0.15	0.2 × 0.14 × 0.06
Data collection			
<i>T</i> _{min} , <i>T</i> _{max}	0.542, 1.000	0.396, 1.000	0.252, 1.000
No. of measured, independent and observed [<i>I</i> > 2σ(<i>I</i>)] reflections	19560, 1048, 998	41673, 1139, 1097	23004, 1260, 1169
<i>R</i> _{int}	0.040	0.034	0.038
(sin θ/λ) _{max} (Å ⁻¹)	0.625	0.625	0.625
Refinement			
<i>R</i> [<i>F</i> ² > 2σ(<i>F</i> ²)], <i>wR</i> (<i>F</i> ²), <i>S</i>	0.018, 0.045, 1.12	0.023, 0.062, 1.13	0.024, 0.068, 1.08
No. of reflections	1048	1139	1260
No. of parameters	47	46	46
No. of restraints	15	0	0
Δρ _{max} , Δρ _{min} (e Å ⁻³)	1.35, -1.37	0.88, -1.28	1.12, -2.54

Table S2. Selected geometric details of Cs₂MHy₂PbX₆ (X = Br, I) at 295 K.

Cs ₂ MHy ₂ PbBr ₆		Cs ₂ MHy ₂ PbBr ₃ I ₃		Cs ₂ MHy ₂ PbI ₆	
Pb1—Br1	3.0186(8)	Pb1—X1	3.1512(7)	Pb1—Br1	3.2098(10)
Pb1—Br1 ⁱ	3.0186(8)	Pb1—X1 ⁱ	3.1513(7)	Pb1—Br1 ⁱ	3.2099(10)
Pb1—Br1 ⁱⁱ	3.0186(8)	Pb1—X1 ⁱⁱ	3.1513(7)	Pb1—Br1 ⁱⁱ	3.2322(8)
Pb1—Br1 ⁱⁱⁱ	3.0186(8)	Pb1—X1 ⁱⁱⁱ	3.1513(7)	Pb1—Br1 ⁱⁱⁱ	3.2321(8)
Pb1—Br2	3.0115(11)	Pb1—Br2	3.0371(11)	Pb1—Br2	3.2322(8)
Pb1—Br2 ⁱ	3.0115(11)	Pb1—Br2 ⁱ	3.0371(11)	Pb1—Br2 ⁱ	3.2322(8)
Br1—Pb1—Br1 ⁱⁱⁱ	94.49(3)	X1—Pb1—X1 ⁱⁱⁱ	94.24(3)	I1—Pb1—I1 ⁱⁱⁱ	94.43(3)
Br1—Pb1—Br1 ⁱⁱ	85.51(3)	X1—Pb1—X1 ⁱⁱ	85.76(3)	I1—Pb1—I1 ⁱⁱ	85.57(3)
Br1 ⁱ —Pb1—Br1 ⁱⁱ	94.49(3)	X1 ⁱ —Pb1—X1 ⁱⁱ	94.24(3)	I1 ⁱ —Pb1—I1 ⁱⁱ	94.43(3)
Br1 ⁱ —Pb1—Br1 ⁱⁱⁱ	85.51(3)	X1 ⁱ —Pb1—X1 ⁱⁱⁱ	85.76(3)	I1 ⁱ —Pb1—I1 ⁱⁱⁱ	85.57(3)
Br2—Pb1—Br1	90.68(2)	Br2—Pb1—X1	91.23(2)	I2—Pb1—I1	90.39(2)
Br2—Pb1—Br1 ⁱ	89.32(2)	Br2—Pb1—X1 ⁱ	88.77(2)	I2—Pb1—I1 ⁱ	89.61(2)
Br2—Pb1—Br1 ⁱⁱⁱ	90.68(2)	Br2—Pb1—X1 ⁱⁱⁱ	91.23(2)	I2—Pb1—I1 ⁱⁱⁱ	90.39(2)
Br2—Pb1—Br1 ⁱⁱ	89.32(2)	Br2—Pb1—X1 ⁱⁱ	88.77(2)	I2—Pb1—I1 ⁱⁱ	89.61(2)
Br2 ⁱ —Pb1—Br1 ⁱ	90.68(2)	Br2 ⁱ —Pb1—X1 ⁱ	91.23(2)	I2 ⁱ —Pb1—I1 ⁱ	90.39(2)
Br2 ⁱ —Pb1—Br1	89.32(2)	Br2 ⁱ —Pb1—X1	88.77(2)	I2 ⁱ —Pb1—I1	89.61(2)
Br2 ⁱ —Pb1—Br1 ⁱⁱ	90.68(2)	Br2 ⁱ —Pb1—X1 ⁱⁱ	91.23(2)	I2 ⁱ —Pb1—I1 ⁱⁱ	90.39(2)
Br2 ⁱ —Pb1—Br1 ⁱⁱⁱ	89.32(2)	Br2 ⁱ —Pb1—X1 ⁱⁱⁱ	88.77(2)	I2 ⁱ —Pb1—I1 ⁱⁱⁱ	89.61(2)
Br1—Pb1—Br1 ⁱ	180.0	X1—Pb1—X1 ⁱ	180.0	I1—Pb1—I1 ⁱ	180.0
Br1 ⁱⁱ —Pb1—Br1 ⁱⁱⁱ	180.0	X1 ⁱⁱ —Pb1—X1 ⁱⁱⁱ	180.0	I1 ⁱⁱ —Pb1—I1 ⁱⁱⁱ	180.0
Br2—Pb1—Br2 ⁱ	180.0	Br2—Pb1—Br2 ⁱ	180.0	I2—Pb1—I2 ⁱ	180.0

Symmetry codes: (i) -x+1, -y+1, -z+1; (ii) x, -y+1, -z+1; (iii) -x+1, y, z.

Table S3. Selected hydrogen-bond parameters of Cs₂MHy₂PbX₆ (X = Br, I) at 295 K.

<i>D</i> —H··· <i>A</i>	<i>D</i> —H (Å)	H··· <i>A</i> (Å)	<i>D</i> ··· <i>A</i> (Å)	<i>D</i> —H··· <i>A</i> (°)
Cs₂MHy₂PbBr₆				
N2—H2A···Br2 ⁱ	0.89	2.46	3.326 (9)	164.2
N2—H2B···Br2 ⁱⁱ	0.89	2.61	3.386 (9)	146.9
N2A—H2AA···Br2 ⁱⁱⁱ	0.89	2.64	3.440 (11)	149.3
N2A—H2AB···Br2 ⁱ	0.89	2.48	3.339 (10)	162.5
Cs₂MHy₂PbBr₃I₃				
N2—H2A···X2 ⁱⁱ	0.89	2.73	3.501 (12)	145.3
N2—H2B···X2 ⁱ	0.89	2.54	3.415 (12)	169.6
N2A—H2AA···X2 ⁱ	0.89	2.53	3.407 (17)	170.2
N2A—H2AB···X2 ⁱⁱⁱ	0.89	2.83	3.59 (2)	144.2
Cs₂MHy₂PbI₆				
N2—H2A···I2 ⁱⁱ	0.89	2.80	3.594 (17)	148.7
N2—H2B···I2 ⁱ	0.89	2.70	3.565 (17)	165.1
N2A—H2AA···I2 ⁱ	0.89	2.70	3.563 (15)	164.8
N2A—H2AB···I2 ⁱⁱⁱ	0.89	2.84	3.629 (16)	149.1

Symmetry code(s): (i) -x+1, -y+1, -z+1; (ii) x, y-1/2, -z+3/2; (iii) -x+1, -y+1/2, z-1/2.

Table S4. Raman wavenumbers of internal modes of MHy^+ (in cm^{-1}) observed for 0D $\text{Cs}_2\text{MHy}_2\text{PbX}_6$, 3D MHyPbBr_3 , 2D $\text{MHy}_2\text{PbBr}_4$ and 1D MHyPbI_3 together with the suggested assignment.^a

$\text{Cs}_2\text{MHy}_2\text{PbBr}_6$	$\text{Cs}_2\text{MHy}_2\text{PbBr}_3\text{I}_3$	$\text{Cs}_2\text{MHy}_2\text{PbI}_3$	MHyPbBr_3 , ¹	$\text{MHy}_2\text{PbBr}_4$, ²	MHyPbI_3	Assignment
3279w	3276w	3278w	3287sh+ 3276vw	3279w	3283w	$\nu_{\text{as}}(\text{NH}_2)$
3236w	3230w	3230w	3217w	3247w	3226m	$\nu_{\text{s}}(\text{NH}_2)$
3165w	3162w	3162w	3164sh+ 3143w	3171w	3151w	$\nu_{\text{as}}(\text{NH}_2^+)$
3115w	3128vw	3110w	3093vw+ 3074vw	3087w	3070w	$\nu_{\text{s}}(\text{NH}_2^+)$
3030sh+3021m	3028sh+3018m	3023sh+3014m	3034sh+ 3027w	3038w+3029 w	3034m+3027m	$\nu_{\text{as}}(\text{CH}_3)$
2957s	2953s	2948s	2950s	2957s	2952s	$\nu_{\text{s}}(\text{CH}_3)$
1607s	1601s	1601s	1593m	1615w	1592m	$\delta(\text{NH}_2)$
1559m	1559m	1552m	1560w	1580m	1559m	$\delta(\text{NH}_2^+)$
1463m+1456m	1460m+1455m	1457m+1449m	1444m	1465sh	1448m+1443m	$\delta_{\text{as}}(\text{CH}_3)$
1446s	1443s	1441s	1432sh	1451s	1435m	$\delta_{\text{as}}(\text{CH}_3)$
1420m	1421m	1418m	1412w	1415w	1411w	$\delta_{\text{s}}(\text{CH}_3)$
	1382w			1378sh		$\omega(\text{NH}_2^+)$
1382w	1373w	1373w	1384w	1361m	1360w	$\omega(\text{NH}_2^+)$
1323m	1321m	1319m	1293m+ 1289m	1321m	1317w	$\tau(\text{NH}_2^+)$
1203w	1202w	1198w	1217m	1202w	1195w	$\rho(\text{CH}_3)+\omega(\text{NH}_2)$
1135s	1135s	1133s	1109m	1139m	1129m	$\tau(\text{NH}_2)+\rho(\text{CH}_3)$
1100w	1098w	1092w	1082m	1097w	1087w	$\rho(\text{CH}_3)+\tau(\text{NH}_2)$

984w+956w	981w	975w+957vw	1002s	989w	975m	$\nu_{as}(\text{CNN})$
888s	886s	881s	871s	891s	878m	$\nu_s(\text{CNN})$
863m+848w	867m	861w+855m	844w	869sh	856m	$\rho(\text{NH}_2^+)$
712w		712w				overtone
436w	435w	431w	449w	450w	441w	$\delta(\text{CNN})$
			309w			MHy-cage mode
				346w	317w	$\tau(\text{NH}_2)$
257w	251w	251w		298vw	249w	$\tau(\text{CH}_3)$

^a key: vs, very strong; s, strong; m, medium; w, weak; vw, very weak; sh, shoulder; b, broad. ν_s , ν_{as} , δ , ρ , ω and τ denote symmetric stretching, antisymmetric stretching, scissoring, rocking, wagging and twisting vibrations. NH_2 and NH_2^+ are terminal and the middle groups in the $\text{CH}_3\text{NH}_2\text{NH}_2^+$ (MHy⁺) cation, respectively.

References:

1. M. Mączka, J. Zienkiewicz and M. Ptak, *J. Phys. Chem. C*, 2022, **126**, 4048-4056.
2. M. Mączka and M. Ptak, *J. Phys. Chem. C*, 2022, **126**, 7991-7998.

Table S5. Raman wavenumbers of lattice modes (in cm^{-1}) observed for 0D $\text{Cs}_2\text{MHy}_2\text{PbX}_6$ and all-inorganic Cs_4PbBr_6 together with the suggested assignment.^a

$\text{Cs}_2\text{MHy}_2\text{PbBr}_6$	$\text{Cs}_2\text{MHy}_2\text{PbBr}_3\text{I}_3$	$\text{Cs}_2\text{MHy}_2\text{PbI}_3$	Cs_4PbBr_6	Assignment
174s	153vs	157s		$T'(MHy^+) + L(MHy^+) + \nu_1$
138sh	120sh		137sh	Overtone
125s	108vs	93vs	124vs	$\nu_1 + T'(MHy^+) + L(MHy^+)$
			107w	ν_2
79s	68m	60s	83vs	ν_5
			75s	ν_5
66vs	56vs	44vs	69vs	$T'(Cs^+) + L(PbX_6)$
59vs			61s+57s	$T'(Cs^+) + L(PbX_6)$
			48s+44s	$T'(Cs^+) + L(PbX_6)$
38m	35m	37m	37m	$T'(Cs^+) + L(PbX_6)$

^a key: vs, very strong; s, strong; m, medium; w, weak; sh, shoulder. ν_1 , ν_2 and ν_5 denote PbX_6 symmetric stretching, antisymmetric stretching and symmetric bending mode, respectively. T' and L stand for translational and librational modes, respectively.

Table S6. Comparison of optical parameters for 0D lead halides.

compound	Structural units, connecting type	absorption (eV)	PL nm (eV)	Stokes shift (nm)	FWHM (nm)	Reference
$\text{Cs}_2\text{MHy}_2\text{PbI}_6$	isolated PbI_6^{4-}	3.14+3.47	637 (1.95)	280	158	This work
Cs_4PbI_6	isolated PbI_6^{4-}	3.38				(i)
		3.38				(ii)
$\text{MA}_4\text{PbI}_6 \cdot 2\text{H}_2\text{O}$	isolated PbI_6^{4-}	3.41				(iii)
$\text{Cs}_2\text{MHy}_2\text{PbBr}_3\text{I}_3$	isolated PbI_6^{4-} and PbBr_6^{4-}	3.33+3.75	680 (1.82)	349	230	This work
$\text{Cs}_2\text{MHy}_2\text{PbBr}_6$	isolated PbBr_6^{4-}	3.73+4.07	647 (1.92)	342	175	This work
Cs_4PbBr_6	isolated PbBr_6^{4-}	3.95				(i)
		3.99				(ii)
		3.77+4.04				This work
$\text{MA}_4\text{PbBr}_6 \cdot 2\text{H}_2\text{O}$	isolated PbBr_6^{4-}	4.00				(iii)
			525 (2.36)	~25	(iv)	
$(\text{C}_3\text{N}_3\text{H}_{11}\text{O})_2\text{PbBr}_6 \cdot 4\text{H}_2\text{O}$	isolated PbBr_6^{4-}	3.74	568 (2.18)	~234	~150	(v)
$\text{Bmpip}_2\text{PbBr}_4$	isolated PbBr_4^{2-}	3.57	470 (2.64)	123	~100	(vi)
$(\text{C}_{13}\text{H}_{19}\text{N}_4)_2\text{PbBr}_4$	isolated PbBr_4^{2-}	3.56	460 (2.70)	111	66	(vii)
$(\text{C}_4\text{H}_8\text{N}_2\text{H}_4)_2\text{PbBr}_6 \cdot 2\text{H}_2\text{O}$	$\text{Pb}_2\text{Br}_{11}^{7-}$, corner-sharing	3.97				(viii)
N-benzylpyridinium ₆ $\text{Pb}_3\text{Br}_{12}$	$\text{Pb}_3\text{Br}_{12}^{6-}$, face-sharing	3.90	571 (2.17)	253	146	(ix)
$(\text{C}_9\text{NH}_{20})_7\text{Pb}_3\text{Br}_{12}$	$\text{Pb}_3\text{Br}_{12}^{6-}$, face-sharing	3.68	522 (2.38)	185	134	(x)
$\text{C}_{12}\text{H}_{30}\text{N}_4\text{Pb}_2\text{Br}_8$	$\text{Pb}_4\text{Br}_{16}^{8-}$, edge-sharing	~3.76	492 (2.52)	~162	182	(xi)
Cs_4PbCl_6	isolated PbCl_6^{4-}	4.37				(i)
		4.36				(ii)
$(\text{C}_9\text{NH}_{20})_7(\text{PbCl}_4)\text{Pb}_3\text{Cl}_{11}$	isolated PbCl_4^{2-} and $\text{Pb}_3\text{Cl}_{11}^{5-}$, face-sharing	3.56	470 (2.64)	122	84	(xii)
$(\text{TAE})_2[\text{Pb}_2\text{Cl}_{10}]\text{Cl}_2$	$\text{Pb}_2\text{Cl}_{10}^{6-}$, edge-sharing	3.77	494 (2.51)	166	263	(xiii)

TAE=tris(2-aminoethyl)ammonium, Bmpip=1-butyl-1-methylpiperidinium

- (i) U. Thumu, M. Piotrowski, B. Owens-Baird and Y. V. Kolen'ko, *J. Solid State Chem.*, 2019, **271**, 361-377.
- (ii) K. A. Akkerman, S. Park, E. Radicchi, F. Nunzi, E. Mosconi, F. De Angelis, R. Brescia, P. Rastogi, M. Prato and L. Manna, *Nano Lett.*, 2017, **17**, 1924-1930.
- (iii) B. A. H. Huisman, F. Palazon and H. J. Bolink, *Inorg. Chem.*, 2021, **60**, 5212-5216.
- (iv) S. K. Sharma, C. Phadnis, T. K. Das, A. Kumar, B. Kavaipatti, A. Chowdhury and A. Yella, *Chem. Mater.*, 2019, **31**, 3111-3117.
- (v) B.B. Cui, Y. Han, B. Huang, Y. Zhao, X. Wu, L. Liu, G. Cao, Q. Du, N. Liu, W. Zou, M. Sun, L. Wang, X. Liu, J. Wang, H. Zhou and Q. Chen, *Nat. Commun.*, 2019, **10**, 5190.
- (vi) V. Morad, Y. Shynkarenko, S. Yakunin, A. Brumberg, R. D. Schaller and M.V. Kovalenko, *J. Am. Chem. Soc.*, 2019, **141**, 9764-9768.
- (vii) H. Lin, C. Zhou, M. Chaaban, L.J. Xu, Y. Zhou, J. Neu, M. Worku, E. Berkwits, Q. He, S. Lee, X. Lin, T. Siegrists, M.H. Du and B. Ma, *ACS Mater. Lett.*, 2019, **1**, 594-598.
- (viii) Y. Takeoka, K. Asai, M. Rikukawa and K. Sanui, *Chem. Lett.*, 2005, **34**, 602-603.
- (ix) B. Febriansyah, C. S. D. Neo, D. Giovanni, S. Srivastava, Y. Lekina, T. M. Koh, Y. Li, Z. X. Shen, M. Asta, T. C. Sum, N. Mathews and J. England, *Chem. Mater.*, 2020, **32**, 4431-4441.
- (x) J. Zhou, M. Li, L. Ning, R. Zhang, M. S. Molokeev, J. Zhao, S. Yang, K. Han and Z. Xia, *J. Phys. Chem. Lett.*, 2019, **10**, 1337-1341.
- (xi) D. Tian, Z. Lai, H. Xu, F. Lin, Y. Jiang, Y. Huang, S. Wang, Y. Cai, J. Jin, R. J. Xie and X. Chen, *Chem. Mater.*, 2022, **34**, 5224-5231.
- (xii) C. Zhou, H. Lin, M. Worku, J. Neu, Y. Zhou, Y. Tian, S. Lee, P. Djurovich, T. Siegrist and B. Ma, *J. Am. Chem. Soc.*, 2018, **140**, 13181-13184.
- (xiii) S. Elleuch, A. Lusson, S. Pillet, K. Boukheddaden and Y. Abid, *ACS Photonics* 2020, **7**, 1178-1197.

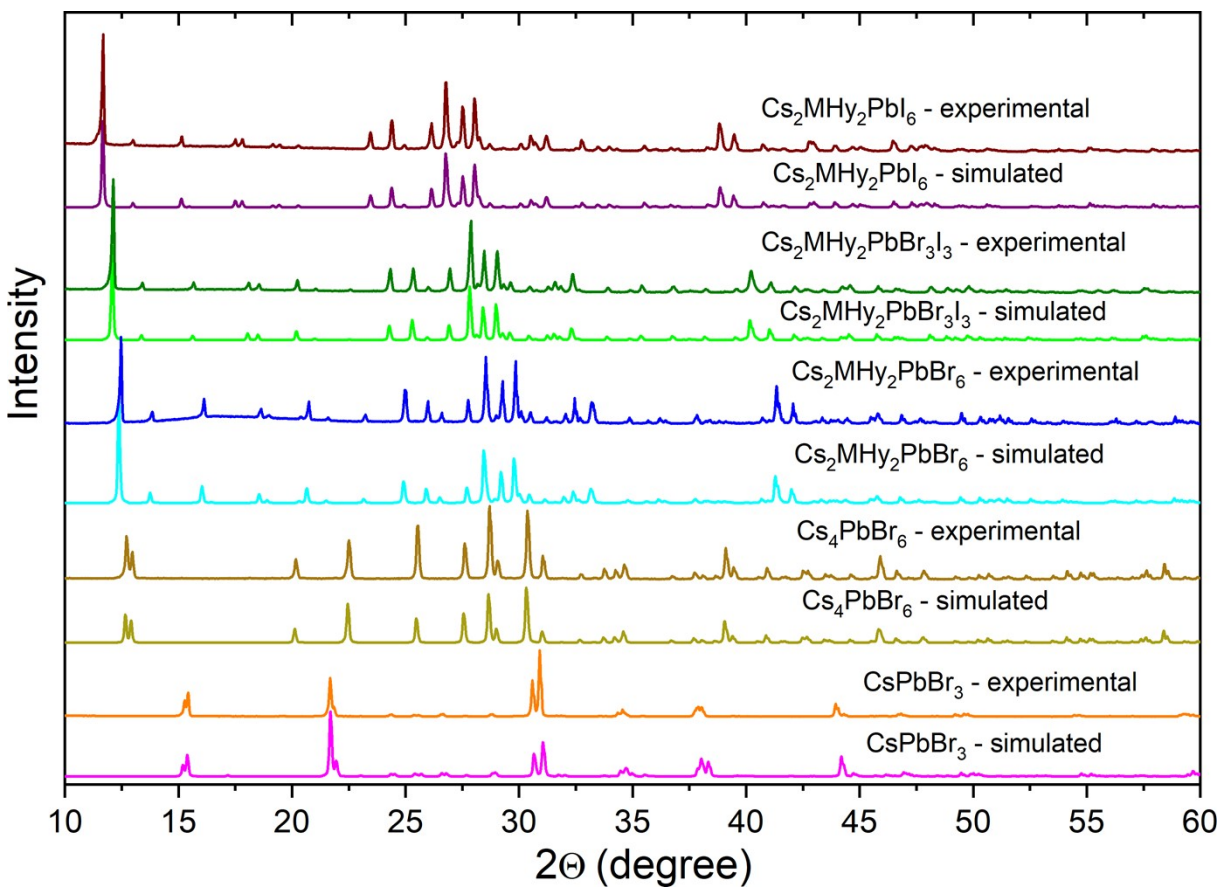


Fig. S1. Powder X-ray diffractograms of the synthesized samples (experimental) together with the simulated ones based on the RT structures.

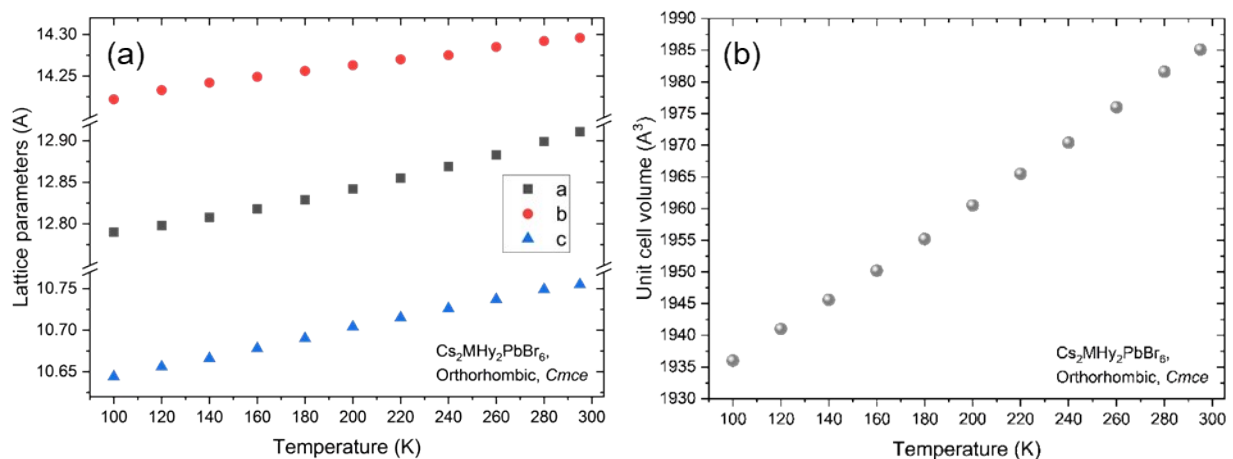


Fig. S2. The temperature evolution of (a) lattice parameters and (b) unit cell volume in $\text{Cs}_2\text{MHy}_2\text{PbBr}_6$.

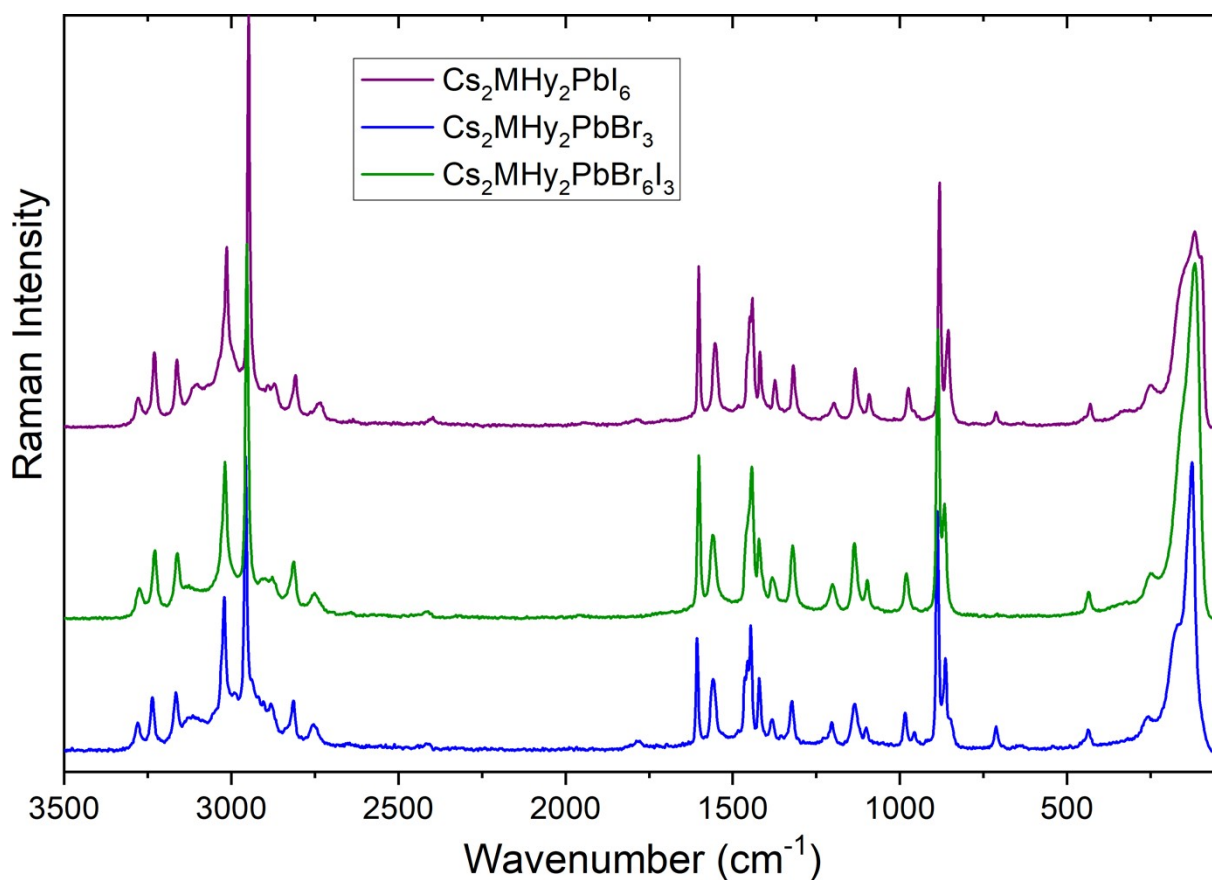


Fig. S3. Raman spectra of $\text{Cs}_2\text{MHy}_2\text{PbX}_6$ compounds in the 3500-100 cm^{-1} range.

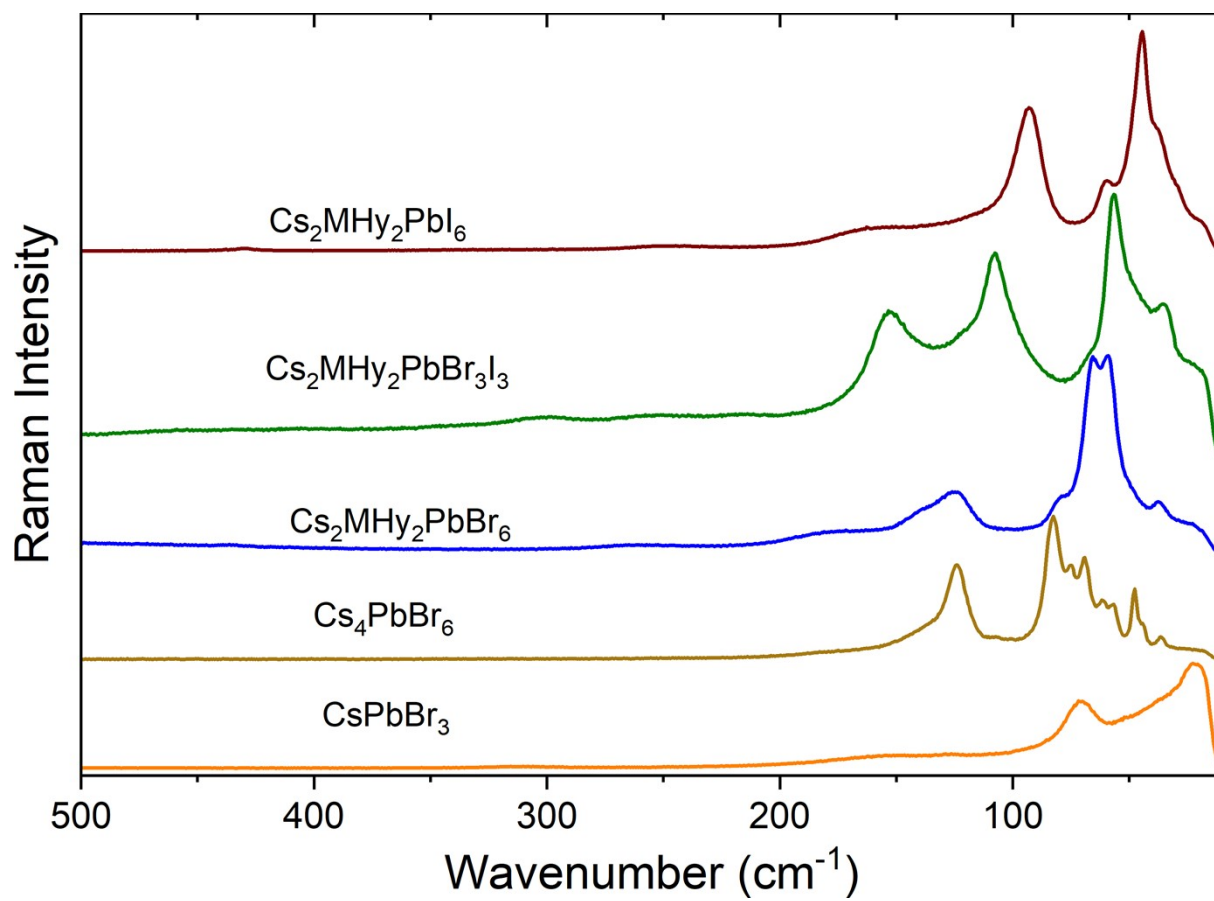


Fig. S4. Raman spectra of Cs₂MHy₂PbX₆ compounds in the 500-10 cm⁻¹ range. For the comparison sake, Raman spectra of all-inorganic CsPbBr₃ and Cs₄PbBr₆ are also shown.

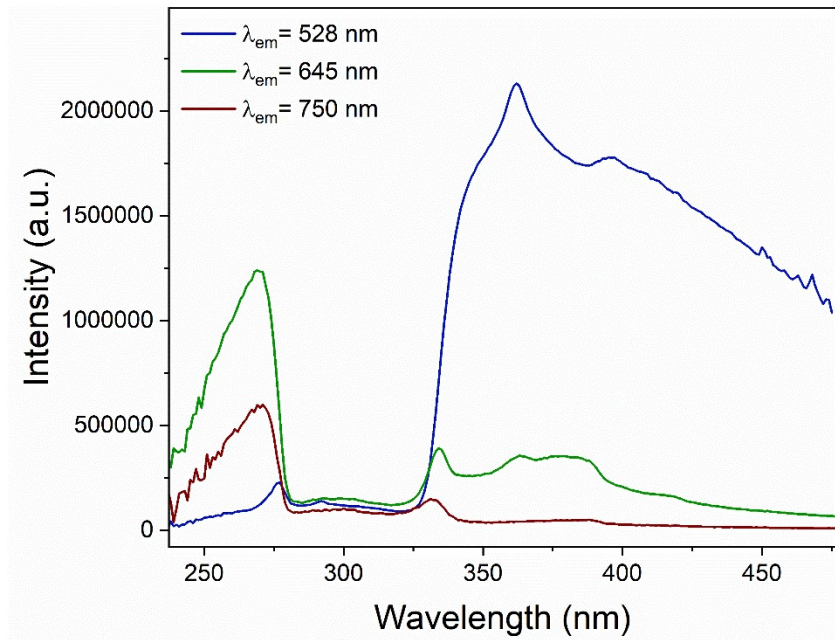


Fig. S5. The emission-wavelength-dependent PL excitation spectra of the representative $\text{Cs}_2\text{MHy}_2\text{PbBr}_6$ sample.

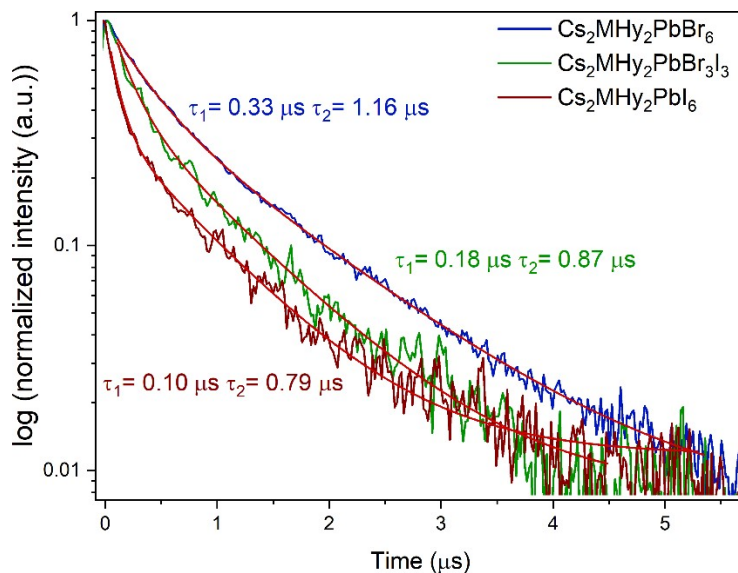


Fig. S6. Low temperature(80 K) emission decay curves of $\text{Cs}_2\text{MHy}_2\text{PbX}_6$ ($X = \text{Br}, \text{I}$) and $\text{Cs}_2\text{MHy}_2\text{PbBr}_3\text{I}_3$ crystals and calculated lifetimes.

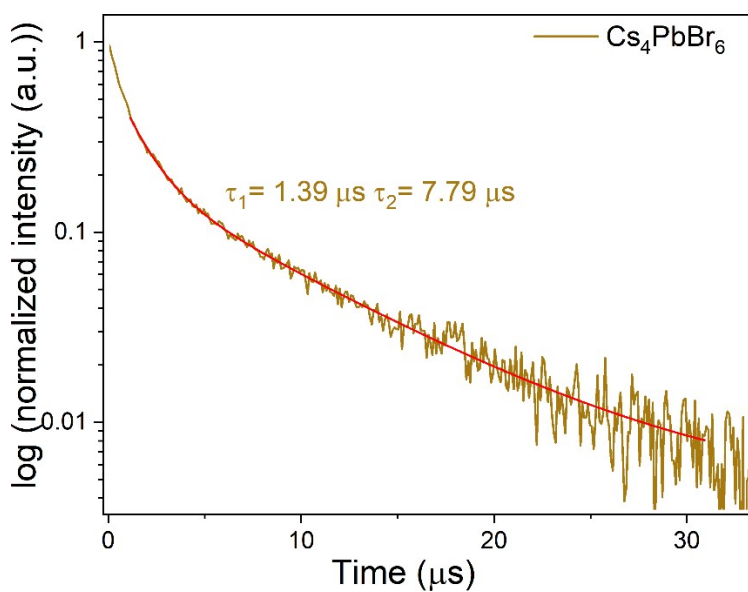


Fig. S7. Low temperature(80 K) emission decay curves of $\text{Cs}_2\text{MHy}_2\text{PbX}_6$ ($X = \text{Br}, \text{I}$) and $\text{Cs}_2\text{MHy}_2\text{PbBr}_3\text{I}_3$ crystals and calculated lifetimes.

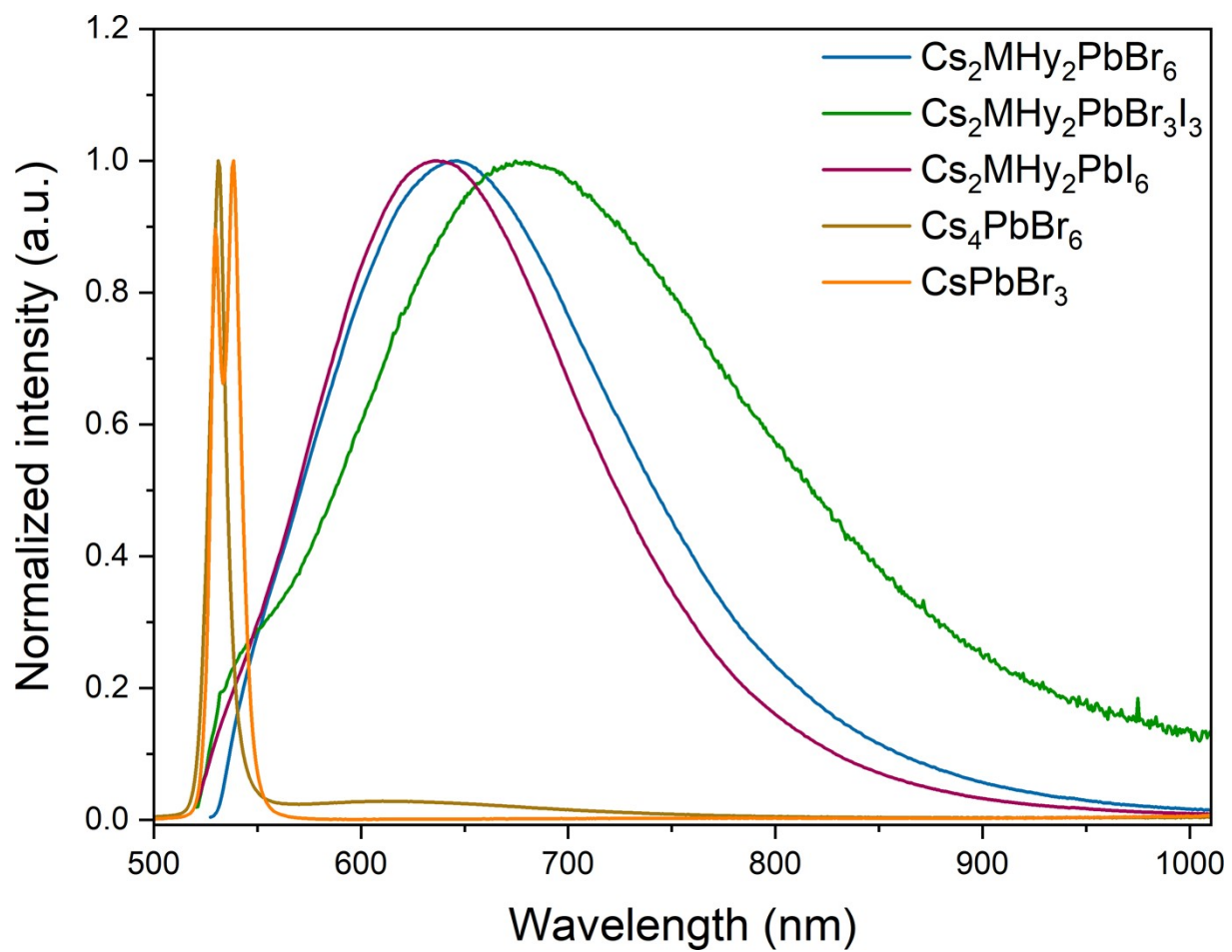


Fig. S8. Collation of the normalized emission spectra of investigated hybrid lead halide perovskites with inorganic Cs_4PbBr_6 and CsPbBr_3 compounds.

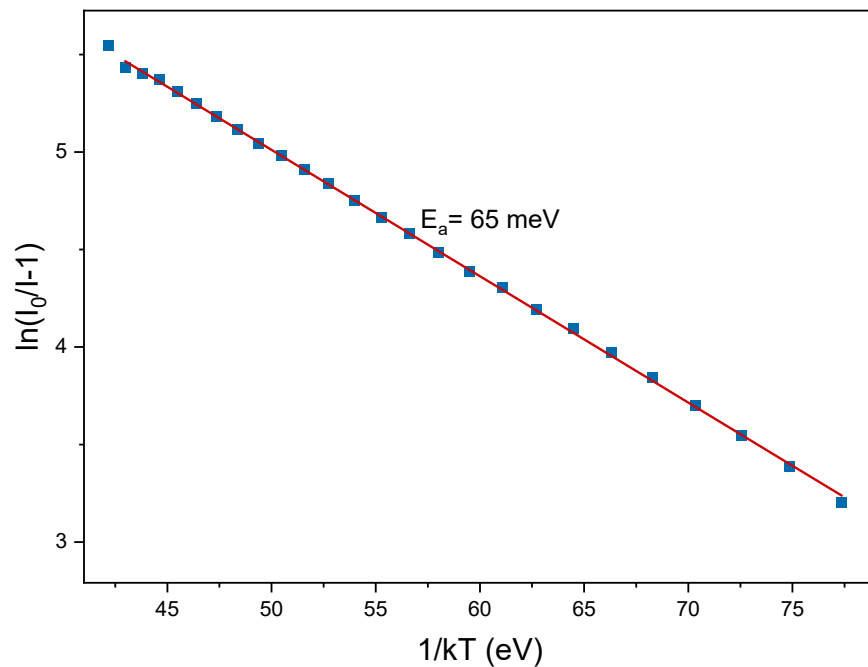


Fig. S9. Logarithm of $I_0/I-1$ as a function of $1/kT$, of $\text{Cs}_2\text{MHy}_2\text{PbBr}_6$. E_a was extracted by fitting the Arrhenius equation.

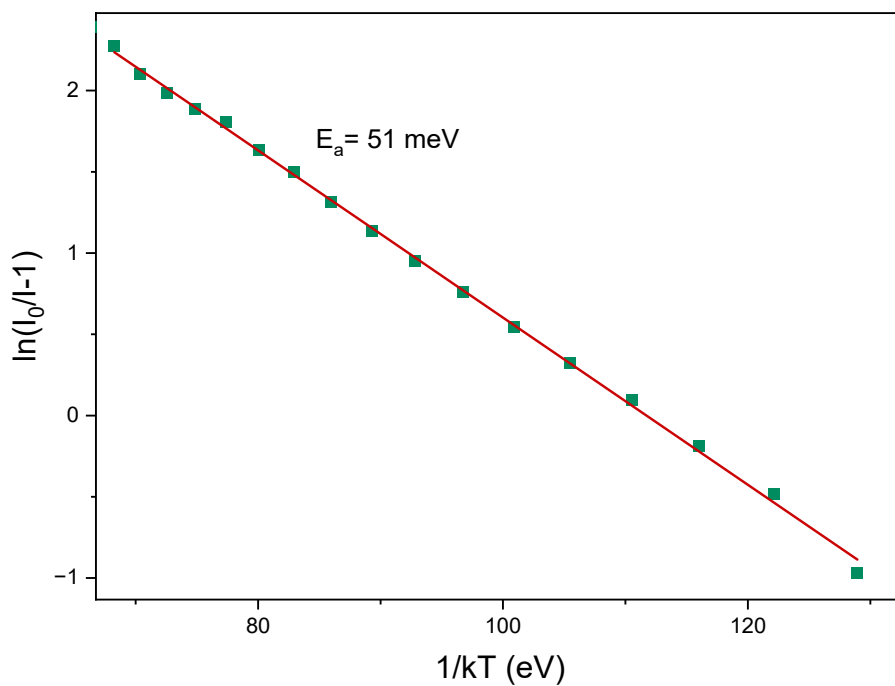


Fig. S10. Logarithm of $I_0/I-1$ as a function of $1/kT$, of $\text{Cs}_2\text{MHy}_2\text{PbBr}_3\text{I}_3$. E_a was extracted by fitting the Arrhenius equation.

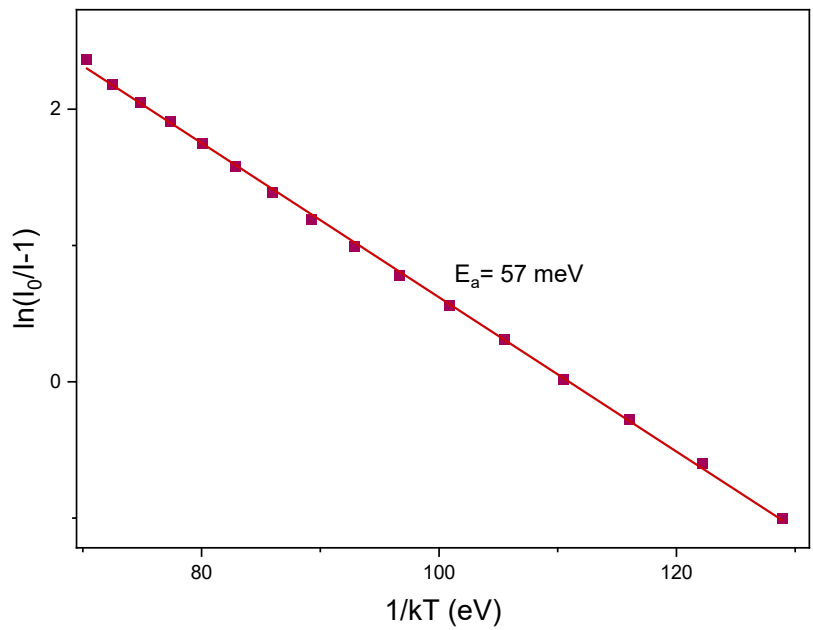


Fig. S11. Logarithm of $I_0/I-1$ as a function of $1/kT$, of $\text{Cs}_2\text{MHy}_2\text{PbI}_6$. E_a was extracted by fitting the Arrhenius equation.